

**Neutron Deformation in  $^{165}\text{Ho}$** 

J. N. Knudson, J. D. Bowman, and S. I. Penttilä

*Los Alamos National Laboratory, Los Alamos, New Mexico 87545*

J. R. Comfort, B. G. Ritchie, J. Goergen, D. Mathis, and J. Tinsley

*Physics Department, Arizona State University, Tempe, Arizona 85287*S. S. Hanna, B. King, and D. Počanić<sup>(a)</sup>*Physics Department, Stanford University, Stanford, California 94305*R. A. Loveman<sup>(b)</sup>*Physics Department, University of Colorado, Boulder, Colorado 80309*

L. S. Fritz and N. S. Dixon

*Physics Department, Franklin and Marshall College, Lancaster, Pennsylvania 17604*

(Received 21 June 1990)

Measurements are reported of orientation asymmetries in the forward-angle differential cross sections for pion single-charge-exchange scattering of aligned and unaligned  $^{165}\text{Ho}$  nuclei. The extrapolated  $0^\circ$  asymmetry of  $-0.022 \pm 0.024$  indicates a quadrupole deformation ratio  $\beta_2^z/\beta_2^y = 0.84 \pm 0.08$ . This result conflicts with the predictions of the best available Hartree-Fock models.

PACS numbers: 21.10.Gv, 21.60.Jz, 25.80.Fm, 27.70.+q

The collective behavior of nucleons and the shapes of nuclei are some of the most basic and intensively studied issues in nuclear physics.<sup>1</sup> Extensive information exists about charge distributions as obtained from electron-scattering, Coulomb-excitation, and muonic-x-ray experiments.<sup>2</sup> However, direct experimental information about neutron distributions is lacking. In the absence of clear evidence to the contrary, an equality between charge ( $\approx$  proton) and neutron distributions is commonly assumed. Although the nuclear symmetry potential acts to maintain similar proton and neutron distributions, the Coulomb potential expands the proton distribution while the neutron distribution is augmented with excess neutrons. The interplay between these competing tendencies is a subject of great importance for models of nuclear structure.

Elastic electron-scattering experiments provide the best systematic information on the nuclear charge distributions. Information on the shapes of the mass (neutron plus proton) distribution may similarly be obtained from the scattering of hadrons. Most methods involve inelastic-scattering experiments and extraction of the matter deformation parameters  $\beta_L$  by use of elaborate reaction calculations based on collective vibrational or rotational models. The analysis is complicated by the finite size of the probes which, when taken into account, tend to reduce discrepancies between the hadronic and electromagnetic results.<sup>3</sup>

In view of the many difficulties, the results of the hadronic experiments are not always consistent. Data for a variety of probes from nucleons through  $^{16}\text{O}$  on a series of targets between  $^{12}\text{C}$  and  $^{28}\text{Si}$  indicate that the mass

and charge deformations are essentially equal.<sup>4</sup> In a similar analysis in the rare-earth region, an equality between the charge and mass deformation parameters near the ends of the region was observed, but sizable differences in between suggested a larger charge than matter quadrupole deformation.<sup>5</sup> However, it was argued in another study for nuclei in the same region that uncertainties in model assumptions precluded definite conclusions about mass and charge shape differences.<sup>6</sup>

Data from inelastic polarized deuteron scattering produced agreement between electromagnetic and nuclear isoscalar transition rates for a variety of spherical nuclei, but showed differences of (10–15)% for several deformed nuclei.<sup>7</sup> It was suggested that nuclei in the latter case had smaller neutron than proton deformations. One of the nuclei was  $^{152}\text{Sm}$ . However, pion-scattering data for which the  $\pi^+$  and  $\pi^-$  are predominantly sensitive to the proton and neutron deformations, respectively, appear to be consistent with equal deformations.<sup>8</sup>

Proton and neutron deformations extracted from electromagnetic and hadronic inelastic-scattering vibrational transitions are theoretically expected to differ for nuclei with  $N \neq Z$  due to the incomplete cancellation of the effects of a neutron excess by the symmetry potential.<sup>9</sup> Such effects have been observed for  $(p, p')$  and  $(n, n')$  reactions on single-closed-shell nuclei.<sup>10</sup> The interesting question of the present study is whether such differences between neutron and proton deformations can be observed in the ground states of permanently deformed nuclei.

In this Letter we present alignment asymmetries based on the measurements of forward-angle cross sections of

single-charge-exchange scattering to the isobaric-analog state of aligned and unaligned  $^{165}\text{Ho}$ . The  $^{165}\text{Ho}$  nucleus has the advantage that it can be aligned with its symmetry axis in a plane perpendicular to the beam direction without the use of an external magnetic field. The present experiment was based on the suggestion of Chiang and Johnson that the orientation asymmetry parameter

$$A_s = \frac{d\sigma^\perp/d\Omega - d\sigma^\parallel/d\Omega}{d\sigma^\perp/d\Omega + d\sigma^\parallel/d\Omega} \quad (1)$$

for the  $(\pi^+, \pi^0)$  charge-exchange reaction at  $0^\circ$  leading to the isobaric-analog state is very sensitive to the ratio  $\beta_2^\perp/\beta_2^\parallel$  of neutral and charge quadrupole deformations.<sup>11</sup> In this equation,  $d\sigma^\parallel/d\Omega$  and  $d\sigma^\perp/d\Omega$  are the differential cross sections for the reaction with the symmetry axis of the deformed nucleus aligned parallel to or perpendicular to the beam direction, respectively. For  $^{165}\text{Ho}$  the parameters of a charged-matter Woods-Saxon distribution having an ellipsoidal surface are  $R_0=6.15$  fm,  $a=0.49$  fm, and  $\beta_2^\parallel=0.32$ .<sup>12</sup>

Chiang and Johnson concluded in a subsequent study that the deformation ratio should also not be very sensitive to uncertainties in the reaction model.<sup>13</sup> Their argument is based on the fact that the transition density in the  $(\pi^+, \pi^0)$  reaction is determined by the spatial distribution of the excess neutrons, that resonance-energy pion reactions probe the nuclear surface, and that the distortions experienced by the pion are the same in both aligned states. This situation is different from that which usually pertains to reaction calculations with light or heavy ions. Specific application to the present experiment has been published recently.<sup>14</sup>

This experiment determined an asymmetry slightly modified from that described in Eq. (1) because the parallel-target orientation is extremely difficult to achieve with the required target geometry. We will thus report asymmetries  $A_r$  for which  $d\sigma^\parallel/d\Omega$  in Eq. (1) is replaced by  $d\sigma/d\Omega$ , the cross section for scattering from a randomly aligned target. Although the sensitivity of  $A_r$  to the deformation is less than that implied by Eq. (1), the experiment is more feasible and reliable.

The data were obtained with 165-MeV pions from the low-energy pion channel at the Clinton P. Anderson Meson Physics Facility (LAMPF). The LAMPF  $\pi^0$  spectrometer<sup>15</sup> was optimized for the detection of 155-MeV  $\pi^0$ 's arising from the reaction  $^{165}\text{Ho}(\pi^+, \pi^0)^{165}\text{Er}$  exciting the isobaric-analog state (IAS).<sup>16</sup> The spectrometer was centered on  $0^\circ$ , with the distance between the target and the first photon conversion plane of each spectrometer arm set to 110 cm. This configuration covered an angular range of about  $12^\circ$  and was used for the entire experiment. The energy resolution for monoenergetic  $\pi^0$ 's was 2.6 MeV (FWHM).

The single-crystal metallic  $^{165}\text{Ho}$  target was composed of two 1.2-mm-thick layers, with the first (second) layer consisting of a tightly packed mosaic of two (three)

pieces of material.<sup>17</sup> All of these pieces were cut in a parallel fashion from a single ingot of high-purity single-crystal  $^{165}\text{Ho}$ , and were placed with the easy magnetization axes in the plane of the large face of the target. The layers were separated by 0.58 cm in order to compensate for the change in the  $\pi^0$  decay opening angle with finite target thickness against the average rate of energy loss in the target.<sup>15,18</sup> The target material was tightly clamped to a large copper frame, which was itself attached to the mixing chamber of a  $^3\text{He}$ - $^4\text{He}$  dilution refrigerator.<sup>19</sup>

A germanium diode resistance thermometer was firmly attached to the copper frame. The target frame was maintained at a temperature of about 70–80 mK with the pion beam incident on the target. A test performed following the experiment confirmed that there was no appreciable temperature difference between the center of the target material and the target frame. At these temperatures, the nuclear-spin axes of the holmium nuclei are almost completely aligned in the basal planes of the crystal lattice,<sup>20</sup> which were aligned perpendicular to the direction of the incident beam (along the  $c$  axis of the crystal). The  $d\sigma^\perp/d\Omega$  data were thus obtained by cooling the target to  $<100$  mK, while the  $d\sigma/d\Omega$  data (i.e., unaligned) required warming the sample to  $>2$  K. All other experimental conditions remained the same, thus minimizing systematic errors.

Cross-section normalizations were obtained by using the LAMPF proton beam current and the activation of scintillator disks as described previously.<sup>16</sup> In addition, an ionization chamber was placed downstream of the cryostat in order to monitor fluctuations in the relative beam fluxes. The relative pion flux between runs could thus be determined to better than 1%. A replica of the cryostat walls, its windows and insulation, and an empty-target frame were used to collect data for target-out subtractions. Data were collected for two complete warm-cold cycles.

The data for each target state were binned into four spectra according to scattering angle. Sample spectra are shown in Fig. 1. The solid angle for each bin was determined by a Monte Carlo simulation<sup>18</sup> of the entire  $\pi^0$  detection process. The spectra were analyzed by using a least-squares-fitting routine, which simultaneously extracts the areas under the IAS peak, the isovector monopole and giant dipole resonances, and a non-resonant background that depends only on the momentum transfer.<sup>21</sup> The line shape for the IAS and the resonances was taken to be a Gaussian central region with exponential tails, which closely reproduces both the experimental line shape for monoenergetic  $\pi^0$ 's and the line shape obtained from Monte Carlo simulations. The shape of the background is fully described in Ref. 21. The location and width of the monopole resonance were fixed to values extrapolated from the systematics established in Ref. 21. The location and width of the dipole resonance were allowed to vary and did not deviate

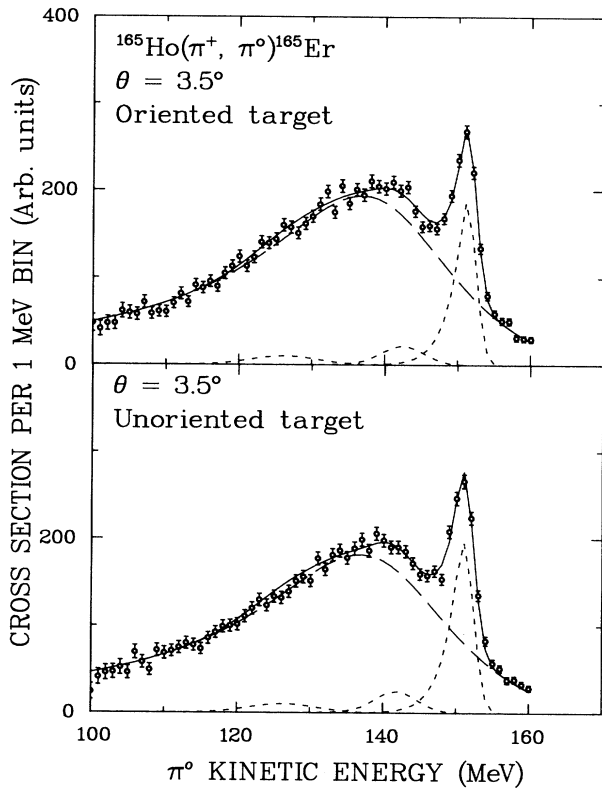


FIG. 1. Spectra of  $\pi^0$  yield at  $3.5^\circ$  for aligned and unaligned targets. The solid curve represents the fit to the data; the long-dashed curve is the  $q$ -dependent background and the short-dashed curves are individual fits to the isovector monopole, giant dipole, and IAS states (left to right).

significantly from the systematics of measured giant dipole resonances. The location and width of the IAS were determined from the data. Typical fits are shown along with the data in Fig. 1. A splitting of the deformed giant dipole resonance (GDR) such as is seen<sup>22</sup> in the analog process  $^{165}\text{Ho}(\gamma, n)$  would be almost completely masked by the spectrometer resolution. Including an allowance for a split GDR in the fitting procedure makes a typically  $< 1\%$  effect on the extracted IAS cross sections. Figure 2(a) shows the extracted asymmetries  $A_r$  as a function of scattering angle.

The IAS cross sections for each target-alignment state were further fitted by the function

$$\sigma(\theta) = a \left[ J_0^2(qR) + \frac{1}{2} (\Delta\theta)^2 \frac{d^2}{d\theta^2} [J_0^2(qR)] \right] \quad (2)$$

as described in Ref. 16, where the overall amplitude  $a$  and the effective scattering radius  $R$  were fitting parameters. The zero-degree alignment asymmetry was determined from the extrapolated values of  $\sigma(0^\circ)$  for the two target states. We obtain  $a = 880 \pm 30$  and  $920 \pm 40$  (arbitrary units), and  $R = 5.9 \pm 0.2$  and  $5.4 \pm 0.2$  fm for the

aligned and unaligned states, respectively. We deduce

$$A_r(0^\circ) = -0.022 \pm 0.024. \quad (3)$$

Equation (2) was also used with the values of  $a$  and  $R$  for the two target states to obtain the functional form of  $A_r(\theta)$  shown in Fig. 2(a).

A value of the ratio  $\beta_n^2/\beta_c^2$  may be extracted from our value of  $A_r(0^\circ)$  by use of the model relationship obtained from the work of Chiang and Johnson,<sup>11</sup> illustrated in Fig. 2(b). This eikonal model is valid only at  $0^\circ$  and therefore does not predict an angular distribution for  $A_r$ . It is believed that the relationship is not very sensitive to parameter ambiguities.<sup>13</sup> We obtain

$$\beta_n^2/\beta_c^2 = 0.84 \pm 0.08. \quad (4)$$

Calculations have also been made with a model that

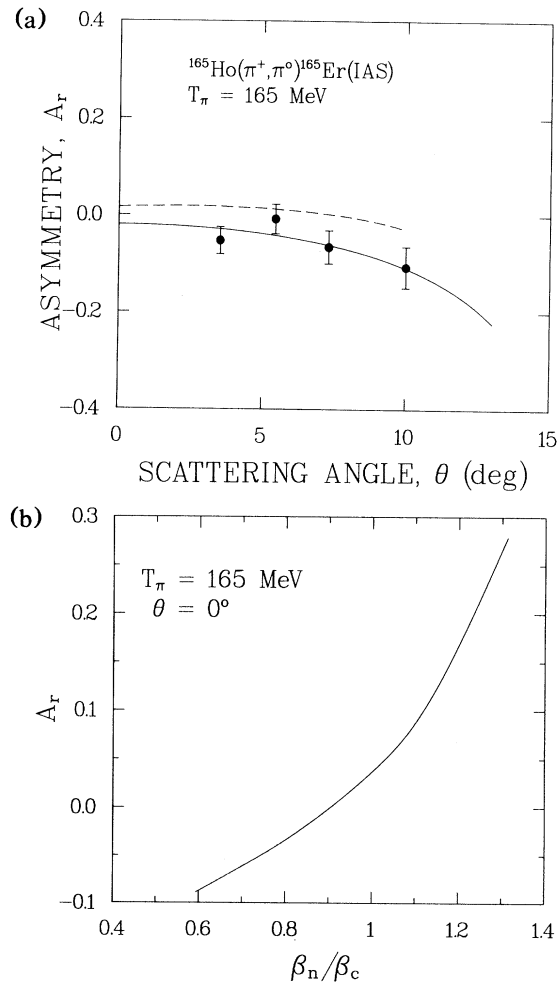


FIG. 2. (a) Measured asymmetries  $A_r$  as a function of scattering angle. The solid curve is a functional form based on Eq. (2). The dashed line gives the result of a coupled-channels calculation of Ref. 14. (b) The eikonal prediction of  $A_r$  as a function of  $\beta_n^2/\beta_c^2$  obtained from Ref. 11.

employs Hartree-Fock densities and a coupled-channels treatment of the reaction mechanism.<sup>14</sup> The dependence of  $A_r(0^\circ)$  on  $\beta_2^n/\beta_2^c$  is believed to be qualitatively similar to that shown in Fig. 2(b), but differs in quantitative detail. However, these calculations have truncation uncertainties brought about by computational limitations. The eikonal results, which do not have such truncations, are perhaps a better representation of the  $0^\circ$  behavior.<sup>14</sup>

On the other hand, the coupled-channels calculations predict an angular distribution that is shown as the dashed curve in Fig. 2(a).<sup>14</sup> Again, the results are quite insensitive to parameter uncertainties.<sup>14</sup> The angular dependence of the asymmetry is similar to the experimental results but the magnitude is more positive than the data. The magnitude is a direct consequence of the fact that the calculation derives from a ratio  $\beta_2^n/\beta_2^c \approx 0.96$ .<sup>14</sup> The Hartree-Fock model calculations produced good agreement with observables such as charge radii and quadrupole moments, and two interactions gave approximately the same value of  $\beta_2^n/\beta_2^c$ .<sup>14</sup> In order to produce good agreement between the experimental and theoretical asymmetries, the relative normalization between the warm and cold data sets would have to be changed by (10–20)%, an amount well outside the statistical and systematic uncertainties of our experiment.

We conclude that the neutron distribution in <sup>165</sup>Ho is considerably less deformed than the charge (proton) distribution, significantly less so than can be computed from the best available Hartree-Fock models. Furthermore, the shape, but not the magnitude of the empirical angular distribution of the alignment asymmetry, agrees with that computed by state-of-the-art coupled-channels methods. These data pose new challenges to models of nuclear structure and reaction mechanisms.

We gratefully acknowledge many useful discussions with Dr. Mikkel Johnson and with Dr. Harvey Marshak. This work was supported by the DOE under Contract No. W-7405-ENG-36 and by the NSF under Grants No. DMR-8507915, No. PHY-8216201, and No. PHY-

8520513.

<sup>(a)</sup>Present address: Department of Physics, University of Virginia, Charlottesville, VA 22901.

<sup>(b)</sup>Present address: Department of Physics, Harvard University, Cambridge, MA 02138.

<sup>1</sup>A. Bohr and B. Mottleson, *Nuclear Structure* (Benjamin, Reading, MA, 1975), Vol. II.

<sup>2</sup>J. L. Friar and J. W. Negele, in *Advances in Nuclear Physics*, edited by M. Baranger and E. Vogt (Plenum, New York, 1975), Vol. 8, p. 219.

<sup>3</sup>D. L. Hendrie, *Phys. Rev. Lett.* **31**, 478 (1973).

<sup>4</sup>W. J. Thompson and J. S. Eck, *Phys. Lett.* **67B**, 151 (1977).

<sup>5</sup>A. B. Kurepin and N. S. Topil'skaya, *Yad. Fiz.* **20**, 1117 (1975) [*Sov. J. Nucl. Phys.* **20**, 585 (1975)].

<sup>6</sup>I. Y. Lee *et al.*, *Phys. Rev. C* **12**, 1483 (1975).

<sup>7</sup>H. Clement *et al.*, *Phys. Rev. Lett.* **48**, 1082 (1982).

<sup>8</sup>C. L. Morris *et al.*, *Phys. Rev. C* **28**, 2165 (1983).

<sup>9</sup>V. R. Brown and V. A. Madsen, *Phys. Rev. C* **11**, 1298 (1975); V. A. Madsen, V. R. Brown, and J. D. Anderson, *Phys. Rev. Lett.* **34**, 1388 (1975); *Phys. Rev. C* **11**, 1298 (1975); **12**, 1205 (1975).

<sup>10</sup>D. E. Bainum *et al.*, *Phys. Rev. Lett.* **39**, 443 (1977).

<sup>11</sup>H.-C. Chiang and Mikkel B. Johnson, *Phys. Rev. Lett.* **53**, 1996 (1984).

<sup>12</sup>R. J. Powers *et al.*, *Phys. Rev. Lett.* **34**, 492 (1975).

<sup>13</sup>H.-C. Chiang and Mikkel B. Johnson, *Phys. Rev. C* **31**, 2140 (1985).

<sup>14</sup>J. Bartel, Mikkel B. Johnson, and M. K. Singham, *Ann. Phys. (N.Y.)* **196**, 89 (1989).

<sup>15</sup>H. W. Baer *et al.*, *Nucl. Instrum. Methods* **180**, 445 (1981).

<sup>16</sup>J. N. Knudson *et al.*, *Phys. Rev. C* **35**, 1382 (1987).

<sup>17</sup>Samples produced by the Materials Preparation Center, Ames Laboratory, Iowa State University, Ames, IA 50011.

<sup>18</sup>S. Gilad, Ph.D. dissertation, Tel-Aviv University, 1979 (unpublished).

<sup>19</sup>T. R. Fisher *et al.*, *Phys. Rev. Lett.* **27**, 1078 (1971).

<sup>20</sup>W. C. Koehler, *J. Appl. Phys.* **36**, 1078 (1965).

<sup>21</sup>A. Erell *et al.*, *Phys. Rev. C* **34**, 1822 (1986).

<sup>22</sup>M. A. Kelly *et al.*, *Phys. Rev.* **179**, 1194 (1969).